Optical Characterization of III-V Multijunction Solar Cells for Temperature-Independent Band Gap Features

Hans Baumgartner, Benjamin Oksanen, Petri Kärhä, and Erkki Ikonen

***Abstract*—A recently developed method to characterize the band gap energies of III-V optosemiconductors was utilized to determine temperature-invariant band gap features of multijunction solar cells. The method is based on measuring electroluminescent spectra of the solar cells at different temperatures. The normalized spectra reveal temperature-invariant energy values of the different junctions which are further converted to band gap energies. The method utilization requires a calibrated spectroradiometer and a temperature controlled mounting base for the solar cell under test, however, no knowledge about the absolute temperature of the cell under measurement. The method was tested on GaAs and GaInP solar cells that consist of single and dual junctions. The band gap energies were also derived from spectral response measurements. The differences of the determined band gap energies from the literature values were smaller than 1.1%. Compared with other band gap determination methods, the developed method yields temperature-invariant band gap characteristics; with a known uncertainty, that separated the different junctions in a multijunction device without individual biasing for the different junctions. In addition, a temperature-independent characterization parameter ensures that the operating conditions of the device under test do not affect the results.**

***Index Terms*—Band gap, light-emitting diode (LED), spectral response, temperature, III-V solar cells.**

I. Introduction

MULTIJUNCTION solar cells (MJSC) based on III-V materials are the third generation of photovoltaic cells, to allow solar energy conversion with efficiencies as high as 46% [1]. In addition to the traditional space applications, recent studies have suggested new applications for high efficiency III-V solar cells in energy harvesting systems. Sensors and devices without batteries or wired power supplies in Internet of Things applications are often utilized in indoor conditions, where ambient light is nowadays produced by use of light emitting diodes (LEDs) or fluorescent lamps. Because of the flexibility of the band gap energy values of III-V solar cells, MJSCs can produce more electricity per surface area under indoor lighting conditions than traditional silicon solar cells. [2]

The band gap energy is an essential parameter to optimize the efficiency and the performance of III-V solar cells. However, in monolithic MJSC, the subcells are not accessible separately, which makes characterization and measurement procedures challenging [3], [4]. Traditional methods to measure the band gap energy of a semiconductor device include techniques based on absorption spectrum [5], ellipsometry [6], photoluminescence [7]–[10], electroluminescence [11], or spectral response [11], [12].

Although the band gap determination techniques mentioned are usable methods to find the material band gap, they have some reported limitations. Band gap determination based on a measured absorption spectrum requires measurement of very small transmittances even below 0.0005 [5]. With use of photoluminescence peaks to determine the material band gap, thermal broadening of the spectrum lowers the precision of the determined band gap at higher temperatures [9]. In addition, the photoluminescence or electroluminescence peak is only an approximation of the band gap energy which, in addition, depends on temperature. In theory, the band gap should not be located at the photoluminescence or electroluminescence peak, however at a lower energy level [10], [13]–[15]. By the use of ellipsometric measurements for band gap determination, the raw ellipsometric measurement data cannot be utilized as such, however additional data analysis and fitting are required to find the material band gap [6]. As the band gap energy is highly temperature dependent, the measurement temperature needs to be well stabilized and known in order to obtain the band gap energy values.

As III-V solar cells are manufactured using effectively the same material compounds and manufacturing processes as III-V light-emitting diodes, they can be used as light-emitting devices as well [15]–[18]. In this article, we present an accurate method to determine temperature-invariant band gap characteristics from the emission spectra of III-V solar cells operated as light-emitting diodes. Emission spectra of a single junction GaAs, a single junction GaInP, and a dual junction GaAs/GaInP sample were measured at varied temperatures and analyzed with a recently published model [19]. The determined band gap characteristics are temperature-invariant, because normalized

Manuscript received April 23, 2019; revised July 1, 2019; accepted July 27, 2019. Date of publication September 9, 2019; date of current version October 28, 2019. This work was supported by projects PV-Enerate and SolCell of EMPIR and EMRP, which are programmes co-financed by the Participating States and the European Union's research and innovation programmes. *(Corresponding author: Hans Baumgartner.)*

H. Baumgartner, B. Oksanen, and P. Kärhä are with the Metrology Research Institute, Aalto University, 02150 Espoo, Finland (e-mail: hans.baumgartner@aalto.fi; benjamin.oksanen@aalto.fi; petri.karha@aalto.fi).

E. Ikonen is with the Metrology Research Institute, Aalto University, 02150 Espoo, Finland, and also with MIKES Metrology, VTT Technical Research Centre of Finland Ltd., 02150 Espoo, Finland (e-mail: erkki.ikonen@aalto.fi).

Color versions of one or more of the figures in this article are available online at http://ieeexplore.ieee.org.

Digital Object Identifier 10.1109/JPHOTOV.2019.2933190

emission spectra intersect at an energy that does not depend on temperature when $T \gg 0\,\mathrm{K}$. This intersection energy can be used as an absolute characterization parameter for the band gap energy of the device under test. The spectra that originate from different junctions of a MJSC were separately analyzed to yield band gap characteristics for each junction. The band gap energies of the corresponding junctions in single and dual junction samples were equal, compared with each other and to literature values, within the measurement uncertainty. We also measured the spectral responses of the solar cells and derived the band gap energies from that data for comparison.

II. Emission Spectrum Model

In this chapter, we describe a mathematical model for the emission spectrum of III-V optosemiconductors, based on a temperature-invariant energy value, applicable to determination of the band gap energies. Authors of this article have developed a novel method to measure the band gap characteristics of light-emitting diodes manufactured using III-V semiconductor materials [19]. That method is here tested and utilized to characterize the band gap energies of an optosemiconductor device that comprise of more than one p-n junction.

An optosemiconductor emits light as a result of spontaneous recombination of electron-hole pairs. The emission intensity at the high-energy slope of the spectrum is given by the product of the joint density of states f and the exponential Boltzmann distribution

$$I\left(E,T\right) = f\left(E - E_g(T)\right) e^{-\frac{E-E_g(T)}{kT}} \tag{1}$$

where E is the photon energy, $E_g(T)$ is the band gap energy at junction temperature T, and k is the Boltzmann constant.

Typically the shift of the band gap energy of an optosemiconductor as a function of temperature is described by the Varshni equation [20]

$$E_g\left(T\right) = E_g\left(0\right) - \frac{\alpha T^2}{T+\beta} \tag{2}$$

where α and β are material Varshni parameters, and $E_g(0)$ is the band gap energy at 0 K. Equation (2) can be expressed as a linear approximation when $T \gg 0$ K [21]

$$E_g(T) \cong E_B - pkT \tag{3}$$

where p is a parameter that defines the linearized band gap energy shift. Equation (2) can be linearized to the form of (3) around temperature T_0 using relations $E_B = E_g(T_0) - E_g'(T_0)T_0$ and $p = -E_g\prime(T_0)/k$, where $E_g\prime$ is the temperature derivative of E_g.

For the joint density of states f in (1), the following functional form [19]:

$$f\left(E - E_g\left(T\right)\right) = r(E - (E_B - pkT))^{p-q} \tag{4}$$

can be derived, where r is a constant, E_B is the temperature-invariant intersection point of the normalized emission spectra, and q is a parameter that defines the shift of the peak energy $E_{\max}(T)$ of the emission spectrum as a function of T. The normalized emission spectra are obtained by division of $I(E,T)$ of (1) with $I(E_{\max}(T),T)$, where $E_{\max}(T)$ is the energy where the intensity is at maximum.

Equation (3) shows that E_B is the linear extrapolation of the temperature dependence of $E_g(T)$ to 0 K [19]. The difference between $E_g(0)$ of (2) and (3) is less than 2% for GaN and GaAs [19], [21]. The extrapolation result does not depend on temperature when $T > 270$ K, hence the temperature dependence of the band gap is linear and can thus be used as an absolute characterization parameter for the band gap energy of the device under test.

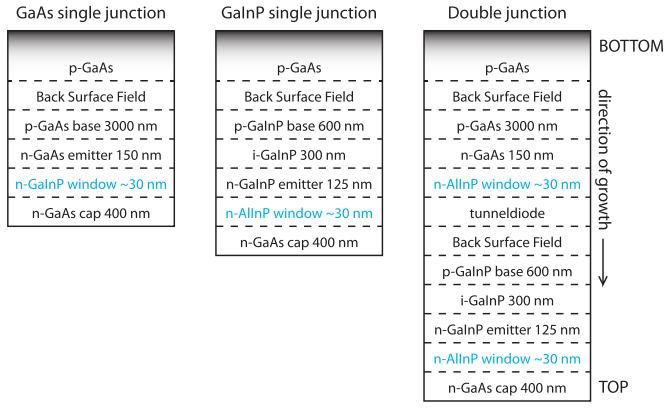

Fig. 1. Layer structures with layer thicknesses of the measured solar cell samples.

III. Experimental

A. Samples

Three different types of III-V solar cells were measured for their spectral responses and emission spectra at varied temperatures. Two of the three samples were single junction solar cells manufactured from GaAs and GaInP. The third sample was a monolithic dual junction cell, comprising of a GaAs and a GaInP junction. All samples were grown by metal-organic vapor phase epitaxy (MOVPE) on a 6° misoriented p-type GaAs substrate. The diameters of the substrates for all three samples were 100 mm, and the epitaxial growth of the layer structures of the samples was performed by MOVPE at Fraunhofer ISE in the same way as in [22].

Fig. 1 shows the layer structures of the three samples. The single junction GaAs and GaInP samples in Fig. 1 consist of a single p-n junction stack of doped GaAs or GaInP on a GaAs substrate. In addition to the p-n junction layer, several other layers are needed to make the semiconductor sample which is an electrically operational solar cell. For ohmic contacts, the p-doped GaAs wafer and the n-doped GaAs cap are used. The window and the back surface field layers near the ohmic contacts reduce unwanted recombination of minority carriers.

The dual junction sample in Fig. 1 is a monolithic cell that consists of GaAs and GaInP p-n junctions connected in series by a tunnel diode. The layer structure and the thicknesses of the layers are the same as in the single junction GaAs and GaInP samples.

The manufactured 100 mm wafers were cut to 10 mm × 15 mm samples, each sample contains 16 individual solar cells. The size of a single solar cell sample was 1.5 mm × 1.5 mm. There were no wires bonded to the samples. However, the back surface was used as a positive contact, and the metallization on top of the cell as a negative contact. To carry out the spectral response and the emission spectrum measurements, the samples were placed on a conductive copper tape, and the tape surface was used to make the electrical contact to the negative terminal. A micropositioner with a tip diameter of 5 μm was used to contact the metallization on top of the cell.

The solar cell samples were fixed on a temperature-controlled mounting base to vary the junction temperatures of the samples during the measurements. The temperature of the mounting base was controlled by the use of a Peltier element and a Wavelength LFI-3550 Peltier controller. The temperature of the mounting base was measured by the use of an AD-590 temperature sensor installed inside the aluminium mounting base. The absolute junction temperature of the device under test was not measured as only the relative change of the junction temperature is needed in our article. The relative change of the junction temperature was assumed to follow the relative change of the heat sink temperature.

B. Spectral Response Measurements

The spectral responses of the single-junction samples were measured for an energy range between 1.3 and 2.5 eV (500–950 nm). A reference spectrometer as in [23] based on a grating monochromator was used to carry out the spectral response measurements. The wavelength step was 1 nm near the band gap energy and 5 nm elsewhere, the bandwidth of the monochromatic light was 2.7 nm. Several measurements were carried out at each wavelength and the average of the measurements was used as the final value.

The spectral responses were measured at three different mounting base temperatures between 280 and 330 K. Assuming that the relatively low light intensity of less than 20 μW of the monochromatic beam did not heat up the sample, the heat sink temperature would be equal to the junction temperature of the solar cell. The samples were allowed a stabilization of 30 min before the measurements. A single spectral response measurement lasted several hours, during which time the temperature of the heat sink varied less than 0.1 K.

The band gap energies of the samples in Fig. 2 were approximated by fitting an exponential function to the data at the band edge and to the saturation region of the spectral response as in [11]. The band gap was derived as the intersection point of the two exponential fits shown in Fig. 2.

Table I shows the determined band gap energies for the samples measured at different temperatures. The exponential fit was fitted to the rising edge of the measurement data between 1% and 50%. The expanded uncertainties in Table I are approximated because of the wavelength uncertainty of 0.5 nm of the measurement device and the effect of the manually chosen modeling limits of the exponential fits.

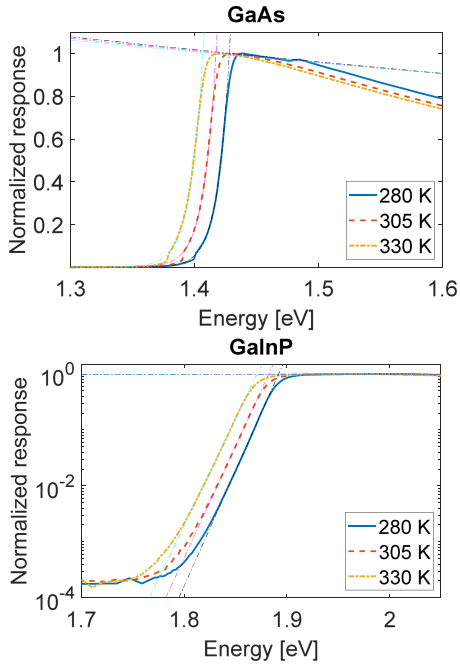

Fig. 2. Spectral responses of the single junction samples measured at different temperatures. The thin dashed lines express exponential fits used to determine the band gap energies.

TABLE I
BAND GAP ENERGIES AND THEIR UNCERTAINTIES (AT 95% CONFIDENCE LEVEL), DETERMINED FROM THE SPECTRAL RESPONSE MEASUREMENTS CARRIED OUT AT DIFFERENT MOUNTING PLATE TEMPERATURES

T	E_g (GaAs) [eV]	E_g (GaInP) [eV]
280 K	1.428 ± 0.008	1.892 ± 0.007
305 K	1.417 ± 0.008	1.882 ± 0.007
330 K	1.407 ± 0.008	1.871 ± 0.007

C. Emission Spectrum Measurements

To determine the band gap energy, emission spectra of the solar cell samples were measured at different temperatures using a temperature controlled mounting base and a spectroradiometer. The temperature of the mounting plate was varied between 270 and 350 K.

Typical current densities in LEDs range from 1 to 100 A/cm^2, which reaches the maximum efficiency at current densities of few A/cm^2. At high (>5 A/cm^2) and low (<1 A/cm^2) current densities, a substantial decrease of efficiency has been demonstrated [24], [25]. At high current levels the decrease of efficiency is tied to the increase in electron leakage current. At low current levels below 1 A/cm^2 the decrease of efficiency is mainly because of the nonradiative electron-hole recombination because of impurities in the depletion region of the junction [13], [26], [27].

The size of the active area of our samples was 1.5 mm × 1.5 mm. With a thermal conductivity of 52 W/(mK) for GaAs we have a thermal resistance of 8.5 W/K for our sample [28]. A driving current of 100 mA (4.4 A/cm^2) was

TABLE II
BAND GAP ENERGIES WITH THEIR UNCERTAINTIES (AT 95% CONFIDENCE LEVEL) OF THE SAMPLES IN eV. PARAMETER E_B DESCRIBES LINEAR EXTRAPOLATION OF THE BAND GAP ENERGY FROM ROOM TEMPERATURE TO 0 K

	GaAs (single junction)	GaAs (double junction)	GaInP (single junction)	GaInP (double junction)
E_B	1.544 ± 0.008	1.545 ± 0.016	2.006 ± 0.006	1.994 ± 0.010
E_g at 305 K from emission spectra	1.413 ± 0.008	1.411 ± 0.016	1.876 ± 0.006	1.872 ± 0.010
E_g at 305 K from spectral response	1.417 ± 0.008	1.416 ± 0.008	1.882 ± 0.007	-
Peak energy at 305 K	1.415 ± 0.003	1.414 ± 0.003	1.878 ± 0.005	1.878 ± 0.005
Literature values of E_g at 305 K	1.42 ± 0.04 [6]	1.42 ± 0.04 [6]	1.887 ± 0.004 [10]*	1.887 ± 0.004 [10]*

*The GaInP band gap literature values are highly sample dependent.

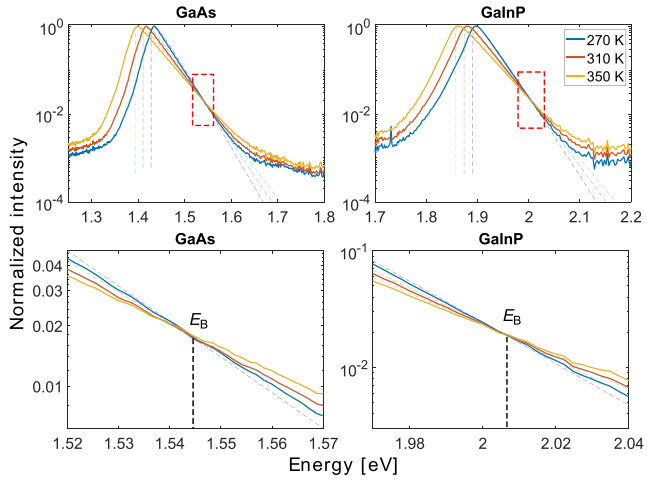

Fig. 3. Measured (solid lines) and fitted (dashed lines) normalized spectra of the single junction GaAs and GaInP samples at different mounting plate temperatures indicated in the figure legend. The lower figures show close ups of the intersection points inside the rectangles.

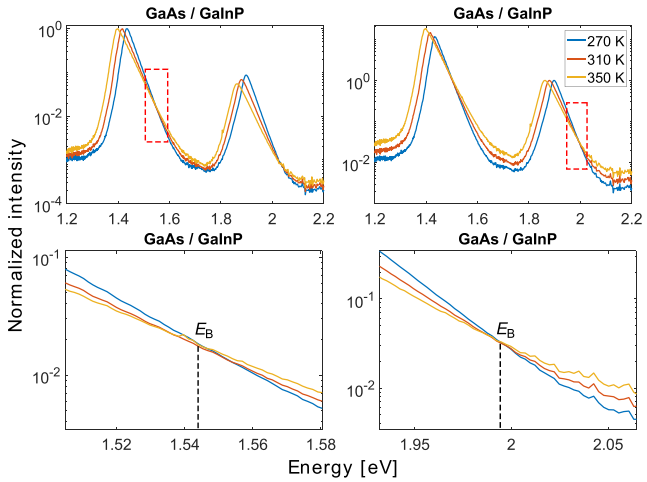

Fig. 4. Emission spectra of the dual junction GaAs/GaInP sample measured at different mounting plate temperatures indicated in the figure legend. In the left figures, the spectra are normalized to the peak intensity of the GaAs junction. In the right figures, the spectra are normalized to the peak intensity of the GaInP junction.

chosen to maximize the efficiency and thus the radiative recombination rate and to provide a reasonable light intensity for the spectroradiometer, still limiting the heating of the sample with the injected current to few kelvins. The calibration of the spectroradiometer is traceable to the spectral irradiance scale of the National Standards Laboratory of Finland [29].

Fig. 3 shows normalized emission spectra of the single junction samples measured at three different temperatures together with curves fitted according to (1) and (4). The curve fitting was made for the spectral ranges close to the peak energy and the intersection point with T given by the mounting plate temperature. As can be seen in Fig. 3, the normalized emission spectra of GaAs and GaInP samples, measured at different temperatures, intersect at energies $E_B = 1.544$ eV and $E_B = 2.006$ eV, respectively. The relative intensity of the intersection points is 0.0193 for both GaAs and GaInP.

Fig. 4 shows normalized spectra for the dual junction GaAs/GaInP sample measured at different temperatures and normalized to both GaAs and GaInP peak intensities. In the case of the dual junction sample, two separate intersection energies exist, one for the GaAs junction and the other for the GaInP junction. The intersection energies can be determined from Fig. 4 to be located at energies 1.545 eV and 1.994 eV, for the GaAs and GaInP peaks, respectively.

IV. ANALYSIS AND DISCUSSION

The band gap energies determined from the emission spectrum and the spectral response measurements of Figs. 2, 3, and 4 are listed in Table II. As the band gap of a semiconductor can be found near the electroluminescence peak, the peak energy is indicated in Table II as well. In addition, the literature values for the band gap energies are listed with references in Table II.

The uncertainty of E_B is determined by the wavelength scale uncertainty of 0.5 nm of the spectroradiometer and the distribution of the intersection points of the normalized spectra at different temperatures. The expanded uncertainty of the peak energy is estimated by the wavelength scale uncertainty of 0.5 nm and wavelength resolution of 0.79 nm of the spectroradiometer.

The band gap energy for GaAs is well characterized in the literature. At 0 K temperature, the band gap energy for GaAs is

(1.517 ± 0.008) eV [6], [28]. Equation (2) with the Varshni parameters of $\alpha = (0.55 \pm 0.13)$ meV/K and $\beta = (225 \pm 174)$ K [6] can then be used to calculate $E_g(305\,\mathrm{K}) = (1.42 \pm 0.04)\,\mathrm{eV}$, which agrees within the stated uncertainties with the values obtained from the emission spectra of GaAs junctions in Table II. Linear extrapolation of the Varshni equation from 305 to 0 K yields a value of 1.56 eV, which deviates less than 1.1% from the intersection energies E_B of the GaAs junctions.

For GaInP junctions, the band gap energy has been reported to be a function of the alloy composition, lattice ordering, and growth temperature [30]. Our sample is known to be of the composition $Ga_{0.5}In_{0.5}P$. Values of ∼1.96 [9] and 1.985 eV [10] have been reported for $E_g(0\,\mathrm{K})$ for such a sample. The latter reference provides information to calculate the linear approximation of the band gap energy around 305 K and to extrapolate the linear approximation to 0 K, which yields $E_B = 1.994$ eV in terms of our parameters. The band gap energy at 305 K is 1.887 eV [10]. The latter two values deviate less than 1% from our results in Table II with both single junction and double junction samples.

Fig. 4 shows that the electroluminescence spectra of GaAs and GaInP junctions are well separated. As long as the number of layers is reasonably low and the band gap energies of the junctions are not too close to each other, the method can be applied to the characterization of different junctions in multijunction cells. At the moment, the most efficient MJSC utilize four p-n junctions with band gap energies of 1.88, 1.42, 1.12, and 0.74 eV, thus the energy differences are similar as in our test results of Fig. 4 [22].

While the emission peaks from different junctions are clearly separable, the effect of luminescent coupling on the emission spectra may affect the results [31]–[33]. The p-n junction of an LED emits photons from both sides of the junction. In a single-junction device the back surface reflects or absorbs photons emitted from the bottom side of the junction. In our double-junction sample, the GaInP junction is on top of the GaAs junction. Some fraction of the photons are emitted towards the GaAs junction, however instead of reflecting back or converting to heat, part of these photons are converted back to electron-hole pairs in the GaAs junction because of luminescent coupling.

The luminescent coupling rates at different temperatures are not constant but depend on the temperature [34], [35]. The effect of the nonconstant coupling rate on the E_B was analyzed from the GaAs emission peak of the double-junction sample. As the spectral data are normalized to the emission peak, only the change of the luminous coupling rate as a function of temperature near the E_B has an influence. The effect of luminescent coupling on the determination uncertainty of E_B is included in the uncertainty in Table II as the variation of the crossing points between different spectra. The variations of the crossing points were smaller than 0.008 eV for all samples.

The interpolated band gap energies at 305 K were calculated by using (3) after parameters p and q were obtained from fitting of the emission spectra according to (1) and (4). With $p = 4.95$ and $p = 4.94$ for the single junction GaAs and GaInP samples, respectively, we got the band gap energy values at 305 K as indicated in Table II. There may be a temperature offset between the mounting plate temperature and the unknown junction temperature T_j, which influences the temperature dependence of the band gap energy values as determined according to (3). In the red InGaAlP LEDs used in [36] and driven with a current of 200 mA, the temperature offset between the mounting base and the p-n junction was around 10 K when the LED was driven with a constant current. When a 1-W LED is being operated, even a short current pulse with a duration of 1 ms will heat up the temperature of the p-n junction by more than 3 K and more than 10 K if the pulse length is 10 ms [37]. The heating of the junction during the current pulse could be overcome by using shorter pulses. However, we have noticed that using pulse lengths shorter than 1 ms may distort the measurement results by changing the shape of the emission spectrum of the LED. In [38] it is suggested that the existence of the temperature-invariant energy value E_B is one way to estimate whether the distortions have changed the operating conditions of the device under test.

As seen in Table II, the band gap energies determined by the use of the emission spectrum measurements and the spectral response measurements agree within the measurement uncertainty, that reveals the reciprocity of the emission spectrum and the quantum efficiency. The measurement results show that the band gap energy values at 305 K of the single junction samples deviate less than 0.4% from the corresponding values of the separate junctions of the double junction sample. Those deviations are smaller than the uncertainty estimates at the 95% confidence level, which indicates that the band gap energies of monolithic multijunction III-V solar cells can be characterized by utilization of the temperature-invariant intersection energy of normalized electroluminescent spectra.

Most of the semiconductor characteristics are highly temperature dependent and determination of the absolute temperature of the p-n junction requires an individual calibration [36], [39]. For high power LEDs, the junction temperature is typically much higher than the heat sink temperature [40]. On the other hand, for GaAs-based optosemiconductors, the junction temperature can be even lower than the temperature of the environment because of the lattice heat converted to photon energy [41]. The temperature invariant intersection energy E_B described in this article is a universal characteristic for III-V single- and multijunction optosemiconductor devices, and it can be measured in a repeatable way, without knowledge about the absolute junction temperature of the device under test.

V. Conclusion

In the case of a multijunction solar cell, characterizing the optical properties of the separate junctions without physical contact to the inner junction is challenging. In addition, most of the material parameters depend on temperature. When characterizing optosemiconductor devices using external bias light or electroluminescent spectra, the external light or driving current can heat up the sample leading to an unknown p-n junction temperature, which deviates from the temperature of the mounting base. We have presented a sensitive method to determine temperature-invariant band gap characteristics from the emission spectra of a multijunction solar cell. Compared with the traditional band gap determination methods based on absorption

spectrum, ellipsometry, photoluminescence, or electroluminescence, our method does not require extremely low signal levels to be measured, uncertainty is determined, and no additional data analysis is required. The band gap energies determined from the emission spectra are in agreement with the literature values and data from spectral response measurements carried out for comparison purposes.

The presented results and method can be utilized as temperature-invariant characterization of III-V solar cells using a simple setup comprising of a spectroradiometer and a temperature controlled mounting base only.

REFERENCES

[1] M. A. Green *et al.*, "Solar cell efficiency tables (Version 50)," *Prog. Photovolt.*, vol. 25, no. 7, pp. 668–676, Jul. 2017.

[2] I. Mathews, P. J. King, F. Stafford, and R. Frizzell, "Performance of III-V solar cells as indoor light energy harvesters," *IEEE J. Photovolt.*, vol. 6, no. 1, pp. 230–235, Jan. 2016.

[3] M. Meusel, R. Adelehelm, F. Dimroth, A. W. Bett, and W. Warta, "Spectral mismatch correction and spectrometric characterization of monolithic III-V multi-junction solar cells," *Prog. Photovolt.*, vol. 10, no. 4, pp. 243–255, Jan. 2002.

[4] H. Nesswetter, N. R. Jost, P. Lugli, A. W. Bett, and C. G. Zimmermann, "Determination of subcell I-V characteristics of multijunction solar cells using optical coupling," *Prog. Photovolt.*, vol. 24, no. 6, pp. 760–773, Jun. 2016.

[5] J. I. Cisneros, "Optical characterization of dielectric and semiconductor thin films by use of transmission data," *Appl. Opt.*, vol. 37, no. 22, pp. 5262–5270, Aug. 1998.

[6] P. Lautenschlager, M. Garriga, S. Logothetidis, and M. Cardona, "Interband critical points of GaAs and their temperature dependence," *Phys. Rev. B*, vol. 35, no. 17, pp. 9174–9189, Jun. 1987.

[7] E. Grill, M. Guzzini, and R. Zamboni, "High-precision determination of the temperature dependence of the fundamental energy gap in gallium arsenide," *Phys. Rev. B*, vol. 45, no. 4, pp. 1638–1644, Jan. 1992.

[8] S. Mukai, "Photoluminescent and electrical properties of InGaPAs mixed crystals liquid phase-epitaxially grown on (100) GaAs," *J. Appl. Phys.*, vol. 54, no. 5, pp. 2635–2645, Jan. 1983.

[9] M. Zachau and W. T. Masselink, "Luminescence and Raman measurement of $In_yGa_{1-y}P$ ($0.3<y<0.5$) grown by gas-source molecular beam epitaxy," *Appl. Phys. Lett.*, vol. 60, no. 17, pp. 2098–2100, Apr. 1992.

[10] Y. Ishitani, S. Minagawa, and T. Tanaka, "Temperature dependence of the band-gap energy of disordered GaInP," *J. Appl. Phys.*, vol. 75, no. 10, pp. 5326–5331, Jan. 1994.

[11] H. Helmers, C. Karcher, and A. W. Bett, "Bandgap determination based on electrical quantum efficiency," *Appl. Phys. Lett.*, vol. 103, pp. 032108-1 – 032108-3, 2013.

[12] W. Hadouchi, J. Rousset, D. Tondelier, B. Geffroy, and Y. Bonnassieux, "Zinc oxide as a hole blocking layer for perovskite solar cells deposited in atmospheric conditions," *RCS Adv.*, vol. 6, pp. 67715–67723, Jul. 2016.

[13] E. F. Schubert, *Light-Emitting Diodes*. Cambridge, U.K.: Cambridge Univ. Press, 2010.

[14] E. E. Perl, J. Simon, J. F. Geisz, M. L. Lee, D. J. Friedman, and M. A. Steiner, "Measurement and modeling of III-V solar cells at high temperatures up to 400°C," *IEEE J. Photovolt.*, vol. 6, no. 5, pp. 1345–1352, Sep. 2016.

[15] C. Karcher, H. Helmers, M. Schachtner, F. Dimorth, and A. W. Bett, "Temperature-dependent electroluminescence and voltages of multijunction solar cells," *Prog. Photovolt.*, vol. 22, pp. 757–763, Jul. 2014.

[16] D. Alonso-Álvarez and N. Ekins-Daukes, "Photoluminescence-based current-voltage characterization of individual subcells in multijunction devices," *IEEE J. Photovolt.*, vol. 6, no. 4, pp. 1004–1011, Jul. 2016.

[17] H. Nesswetter, P. Lugli, A. W. Bett, and C. G. Zimmermann, "Electroluminescence and photoluminescence characterization of multijunction solar cells," *IEEE J. Photovolt.*, vol. 3, no. 1, pp. 353–358, Jan. 2013.

[18] T. Kirchartz *et al.*, "Internal voltages in GaInP / GaInAs / Ge multijunction solar cells determined by electroluminescence measurements," *Appl. Phys. Lett.*, vol. 92, no. 12, Mar. 2008, Art. no. 123502.

[19] H. Baumgartner, A. Vaskuri, P. Kärhä, and E. Ikonen, "Temperature invariant energy value in LED spectra," *Appl. Phys. Lett.*, vol. 109, no. 23, Nov. 2016, Art. no. 231103.

[20] Y. P. Varshni, "Temperature dependence of the band gap in semiconductors," *Physica*, vol. 34, pp. 149–154, 1967.

[21] A. Keppens, W. R. Ryckaert, G. Deconick, and P. Hanselaer, "High power light-emitting diode junction temperature determination from current voltage characteristics," *J. Appl. Phys.*, vol. 104, no. 9, Sep. 2008, Art. no. 093104.

[22] F. Dimroth *et al.*, "Wafer bonded four-junction GaInP/GaAs//GaInAsP/GaInAs concentrator solar cells with 44.7% efficiency," *Prog. Photovolt.*, vol. 22, no. 3, pp. 277–282, Mar. 2014.

[23] F. Manoochehri *et al.*, "Characterization of optical detectors using high-accuracy instruments," *Anal. Chim. Acta*, vol. 380, no. 2, pp. 327–337, Feb. 1999.

[24] I. V. Rozhanksy and D. A. Zakheim, "Analysis of process limiting quantum efficiency of AlGaInN LEDs at high pumping," *Phys. Status Solids*, vol. 204, no. 1, pp. 227–230, Jan. 2007.

[25] M.-H. Kim *et al.*, "Origin of efficiency droop in GaN-based light-emitting diodes," *Appl. Phys. Lett.*, vol. 91, no. 18, Oct. 2007, Art. no. 183507.

[26] S. Roensch, R. Hoheisel, F. Dimroth, and A.W. Bett, "Subcell I-V characteristics analysis of GaInP/GaInAs/Ge solar cells using electroluminescence measurements," *Appl. Phys. Lett.*, vol. 98, Jun. 2011, Art. no. 251113.

[27] A. L. Fahrenbruch and R. H. Bube, *Fundamentals of Solar Cells*. New York, NY, USA: Academic, 1983.

[28] J. S. Blakemore, "Semiconducting and other major properties of gallium arsenide," *J. Appl. Phys.*, vol. 53, no. 10, pp. R213–R181, May. 1982.

[29] T. Kübarsepp *et al.*, "Spectral irradiance measurements of tungsten lamps with filter radiometers in the spectral range 290 nm to 900 nm," *Metrologia*, vol. 37, no. 4, pp. 305–312, 2000.

[30] T. Suzuki *et al.*, "Band-gap energy anomaly and sublattice ordering in GaInP and AlGaInP grown by metalorganic vapor phase epitaxy," *Jpn. J. Appl. Phys.*, vol. 27, no. 11, pp. 2098–2109, Nov. 1988.

[31] C. Baur, M. Hermle, F. Dimroth, and A. W. Bett, "Effects of optical coupling in III-V multilayer systems," *Appl. Phys. Lett.*, vol. 90, May 2007, Art. no. 192109.

[32] D. Derkacs, T. Bilir, and V. A. Sabnis, "Luminescent coupling in GaAs/GaInNAsSb multijunction solar cells," *IEEE J. Photovolt.*, vol. 3, no. 1, pp. 520–527, Jan. 2013.

[33] M. A. Steiner and J. F. Geisz, "Non-linear luminescent coupling in series-connected multijunction solar cells," *Appl. Phys. Lett.*, vol. 100, Jun. 2012, Art. no. 251106.

[34] D. J. Friedman, J. F. Geisz, and M. A. Steiner, "Analysis of multijunction solar cell current-voltage characteristics in the presence of luminescent coupling," *IEEE J. Photovolt.*, vol. 3, no. 4, pp. 1429–1436, Oct. 2013.

[35] D. J. Friedman, "Modelling of tandem cell temperature coefficients," in *Proc. 25th IEEE Photovolt. Spec. Conf.*, 1996, pp. 89–92.

[36] A. Vaskuri, H. Baumgartner, P. Kärhä, G. Andor, and E. Ikonen, "Modeling the spectral shape of InGaAlP-based red light-emitting diodes," *J. Appl. Phys.*, vol. 118, no. 20, Nov. 2015, Art. no. 203103.

[37] *Optical Measurements of High-Power LEDs*, CIE 225:2017, International Commission on Illumination, Vienna, Austria, 2017.

[38] A. Vaskuri *et al.*, "Relationship between junction temperature, electroluminescence spectrum and ageing of light-emitting diodes," *Metrologia*, vol. 55, pp. S86–S95, 2018.

[39] Y. Xi *et al.*, "Junction and carrier temperature measurement in deep-ultraviolet light-emitting diodes using three different methods," *Appl. Phys. Lett.*, vol. 86, no. 3, Nov. 2005, Art. no. 031907.

[40] A. Keppens, W. R. Ryckaert, G. Deconinck, and P. Hanselaer, "Modeling high power light-emitting diode spectra and their variation with junction temperature," *J. Appl. Phys.*, vol. 108, no. 4, Jun. 2010, Art. no. 043104.

[41] G. C. Dousmanis, C. W. Mueller, H. Nelson, and K. G. Petzinger, "Evidence of refrigerating action by means of photon emission in semiconductor diodes," *Phys. Rev.*, vol. 133, no. 1A, pp. A316–A318, Jan. 1964.